Implementation of Distributed-Parameter Model of Power Cable in PSCAD/EMTDC Software

Thiago F. L. Milagres, Alessandro F. Moreira, Wallace C. Boaventura, Hélder de Paula
Departamento de Engenharia Elétrica, UFMG. Belo Horizonte - MG - Brasil
Tel: +55 (31) 3409-4840 Email: moreira@cpdee.ufmg.br

Abstract **The Electromagnetic Transients (*EMTP*) based programs are suitable for cable modeling in modal and phase domains. However, these models are intended to analyze electromagnetic transients when high-voltage cables are used in underground and overhead power systems. This work aims to develop a computational model of power cable placed on the ground surface and in trays for electrical drive applications. These models include the distributed-nature and frequency-dependent parameters of the cable. Such modeling, which is developed to be used in the $PSCAD/EMTDC^{©}$ software, is very useful to analyze the over-voltage phenomena in pulse width modulated (*PWM*) drives, for both low and medium voltage levels. Simulation and experimental results come along validating the computational models.**

Index Terms Industrial Drives; Overvoltage in Long Cable Drives; PSCAD/EMTDC Models.

I. Introduction

As the technology has progressed in the application of pulse width modulation (PWM) inverters over past decades, the switched-power devices used in these inverters also have been greatly improved, resulting faster switching rates. Moreover, in several industrial plants the cable connecting the converter and the machine may have a length of some hundreds of meters, resulting in problems both in the converter and in the machines, such as the overvoltage phenomena [1], [2], [3], [4], [5].

In the last decade many works have been addressed the overvoltage phenomena, proposing not only system models, but also solutions to overcome the related problems [6], [7], [8]. The present work has the objective to improve the model that is used to represent the power cable. Traditionally, many works have suggested the use of lumped-parameter representation. Single or multi-phase lines can be modeled. A simple lumped-parameter section model will give the correct fundamental line impedance, but cannot accurately represent other frequencies unless many sections are used [9].

On the other hand, a distributed-representation of the transmission line, which is most suited for transient line response, is much more convenient than the lumped-parameter representation to model the power cable. A distributed model operates on the principle of traveling waves. A voltage disturbance will travel along a conductor at its propagation velocity (near the speed of light), until it is reflected at the lines end. In a sense, a transmission line or cable is a delay function. Whatever is fed into one end will appear at the other end, perhaps slightly distorted, after some delay. However, there are some other considerations which must be dealt which include mutual coupling with other conductors, and wave-shape attenuation as it travels along the line. The frequency-dependent line model represents the frequency dependence of all parameters. This model is necessary for studies requiring a very detailed representation of the line over a wide frequency range. Frequency-dependent models can be solved using modal techniques [10], [11], [12] or using more advanced phase domain techniques [13], [14]. Although, the phase domain model be numerically robust and more accurate than any other commercially available line/cable model, in the case of system configuration (symmetric, balanced and transposed throughout its length) considered in this paper, the frequency dependent modal domain model should thus be preferred to represent all frequency dependent effects of the cable, including the skin effect (line resistance increases with frequency) and the modal transformation matrices frequency dependent effects.

In order to use the distributed-representation of the transmission line, the electromagnetic transient softwares are required, such as the PSCAD/EMTDC [15]. However, these programs do not have suitable models for power cable utilized in drive applications, which connect converters and motors through trays or above ground. In this context appears the present work. The main goal of this paper is to develop aforementioned models for power cables to study overvoltage related problems using EMTP based programs. Experimental analysis of the model is presented to validate the model. Simulation and experimental results of the overvoltage come along demonstrating the suitability of the computational models.

II. Distributed-Parameter Model of the Cable

The development of the computational model to be used in the PSCAD/EMTDC program is realized in three steps:

- *Estimation of the power cable parameters* – Usually, measurement of the parameters is not straightforward. Therefore, a set of equations based on the physical and geometric characteristics of the cable are used to carried out the series impedance and the propagation function, both frequency dependent.
- *Synthesis of the rational functions* – Since the PSCAD/EMTDC does not have a dedicated model of the power cable, the idea is to use its computational platform to carried out the transients results. Therefore, it is necessary to change the rational function that represent

the series impedance (*i.e.* poles, residues and gain) and the propagation function (*i.e.* poles and residues). In consequence, the dynamic characteristics of the model is changed.

- *Implementation of the system in the time domain* – Since the rational functions that represent the series impedance and the propagation function are carried through, the implementation of the power cable model in the PSCAD/EMTDC computational platform can be done and calculation of the electrical transients in the time domain can also be carried out.

A. *Estimation of the power cable parameters*

The power cable model is developed for two situations: cables placed over the ground and placed in trays. In this two situations the cable is a four wire unshielded cable. The following parameters are estimated: series impedance, shunt admittance, characteristic impedance and propagation factor in the modal domain.

The series impedance can be calculated by expression (1), where $R(\omega)$ is a frequency dependente resistance including the intrinsic resistance of the conductors and earth returning resistance through the ground; and $L(\omega)$ is a frequency dependent inductance, including the self inductance of the conductors, the mutual inductance between the conductors and the earth returning inductance through the ground.

$$Z(\omega) = R(\omega) + j\omega L(\omega). \tag{1}$$

The series impedance can be also represented by expression (2), where $Z_{int}(\omega)$ is the internal impedance of the condutor, which includes the skin effect estimation, and $Z_{ext}(\omega)$ is the external impedance of the conductor, which includes the geometric characteristics of the conductor referred to the ground, as well as the earth return characteristics.

$$Z(\omega) = Z_{int}(\omega) + Z_{ext}(\omega), \tag{2}$$

The skin effect contribution in the internal impedance ($Z_{int}(\omega)$) is usually express by Bessel series [16]. However, theses functions generally presents problems of precision and convergence [17]. To overcome these drawbacks, the analytic solution presented by equation (3) is utilized, with 6,6 % maximum error [18]:

$$Z_{int}(\omega) = \sqrt{n^2 + m^2}, \tag{3}$$

where:

$n = \frac{1}{\pi r^2 \sigma_c}$;
$m = \frac{1}{2\pi\sigma_c r p}$;
$p = \frac{1}{\sqrt{\omega\mu_0\sigma_c}}$;
$\mu_0 = 4\pi 10^{-7}$;
$\sigma_c = \frac{1}{\rho_c}$;
r - conductor radius;
ρ_c - conductor resistivity (Ωm).

In the technical literature there are many different methods to calculate the ground return impedance [16], [19], [20] and some studies comparing theses methods [21], [22]. In this paper, the authors had chosen the method developed by Deri [23] (Figure 1), with some adaptations for the power cable modeling.

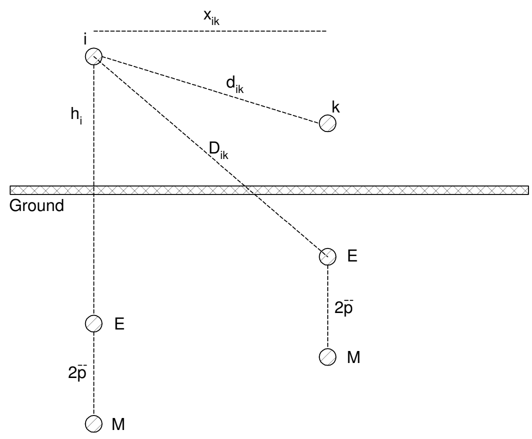

Fig. 1. Method developed by Deri that takes into account the complex depth. Where E, M and $\overline{p}$ correspond respectively to the electrical image, to the magnetic image and to the complex depth.

The main difference between the original method formulated by Deri and the model presented in this paper is the parcel "-r" that was added to the impedance and admittance equations. The inclusion of the parcel "-r" in the equations (4), (5), (6) and (7) can be justified because, in the actual modeling, the values of the distances between two conductors and the conductors and the ground (of the order of some millimeters) are close to the geometric rays values of the conductors, which do not occur in the transmission lines modeling.

Thus, the series impedance $Z_{ext}(\omega)$ can be divided in two equations. The first one represents the self impedance of the conductor (equation 4). The second one represents the impedance between two conductors (equation 5):

$$Z_{ext-kk}(\omega) = R_i + j\omega\frac{\mu_0}{2\pi}\ln\frac{2(h_i + \overline{p}) - r}{r}, \tag{4}$$

$$Z_{ext-ki}(\omega) = j\omega\frac{\mu_0}{2\pi}\ln\frac{\sqrt{(h_i + h_k + 2\overline{p})^2 + x_{ik}^2} - r}{d_{ik} - r}, \tag{5}$$

where:

$\overline{p} = \sqrt{\frac{\rho_t}{\omega\mu_0}}$;
ρ_t - ground resistivity (Ωm);
R_i - the d.c. resistance (Ω/m);
r - external radius of the conductor.

The capacitances matrix is assembled taking in account the capacitance between the conductors and the ground (equation 6), and the capacitance between the conductors, as shown by equation (7):

$$C_{c-t} = \frac{2\pi\epsilon_0}{\ln\left(\frac{2h_i - r}{r}\right)}, \tag{6}$$

$$C_{c-c} = \frac{\pi \epsilon_0 \epsilon_r}{\ln\left(\frac{d_{ik}-r}{r}\right)}. \quad (7)$$

The elements of the capacitance matrix main diagonal C_{ii} represent all the capacitances related to the conductor *i*. On the other hand, the elements that do not belong to the main diagonal represent the capacitance between the conductors *i* and *k*, with negative signal.

The shunt admittance can be calculated by equation (8), which includes the estimation of the capacitance between the conductors and the capacitance between conductor and ground. In the case of power cable modeling, the "$shunt$" conductance *G*(S/m)is very small, therefore it was be neglected.

$$[Y(\omega)] = j\omega[C]. \quad (8)$$

The final result for the series impedance and the shunt admittance for the four wire cable are matrices, as shown by equations (9) and (10), respectively.

$$[Z(\omega)] = \begin{bmatrix} Zs(\omega) & Zm(\omega) & \dots & Zm(\omega) \\ Zm(\omega) & Zs(\omega) & \dots & Zm(\omega) \\ \vdots & \vdots & \ddots & \vdots \\ Zm(\omega) & Zm(\omega) & \dots & Zs(\omega) \end{bmatrix}, \quad (9)$$

where $Zs(\omega) = Z_{int}(\omega) + Z_{ext-kk}(\omega)$ and $Zm(\omega) = Z_{ext-ki}(\omega)$.

$$[Y(\omega)] = \begin{bmatrix} Ys(\omega) & Ym(\omega) & \dots & Ym(\omega) \\ Ym(\omega) & Ys(\omega) & \dots & Ym(\omega) \\ \vdots & \vdots & \ddots & \vdots \\ Ym(\omega) & Ym(\omega) & \dots & Ys(\omega) \end{bmatrix}, \quad (10)$$

where $Ys(\omega) = j\omega(C_{ii})$ and $Ym(\omega) = -j\omega(C_{ik})$.

The next step is to calculate the characteristic impedance and propagation factor in the modal domain, based on the series impedance and shunt admittance matrices. Herein, a Clarke transformation is used, which is more suitable to evaluate electromagnetic transients, especially for the case studied in this paper [16]. The transformation that is utilized in this work is shown by equation (11).

$$[T] = \begin{bmatrix} \frac{1}{\sqrt{4}} & \frac{1}{\sqrt{2}} & \frac{1}{\sqrt{6}} & \frac{1}{\sqrt{12}} \\ \frac{1}{\sqrt{4}} & -\frac{1}{\sqrt{2}} & \frac{1}{\sqrt{6}} & \frac{1}{\sqrt{12}} \\ \frac{1}{\sqrt{4}} & 0 & -\frac{2}{\sqrt{6}} & \frac{1}{\sqrt{12}} \\ \frac{1}{\sqrt{4}} & 0 & 0 & -\frac{3}{\sqrt{12}} \end{bmatrix}. \quad (11)$$

Using the transformation as suggested, it is obtained the series impedance and the shunt admittance in the modal domain, as shown by equations (12) and (13), remembering that for balanced systems the voltage and current transformations are the same, that is $[T_v] = [T_i] = [T]$.

$$[Z_{mod-i}(\omega)] = [T_v]^{-1} \cdot [Z(\omega)] \cdot [T_i]. \quad (12)$$

$$[Y_{mod-i}(\omega)] = [T_i]^{-1} \cdot [Y(\omega)] \cdot [T_v]. \quad (13)$$

Therefore, the characteristic impedance and propagation factor in the modal domain can be calculated by the expressions (14) and (15):

$$[Z_{c-mod-i}(\omega)] = \sqrt{\frac{[Z_{mod-i}(\omega)]}{[Y_{mod-i}(\omega)]}}, \quad (14)$$

$$[A_{mod-i}(\omega)] = e^{-[\gamma_{mod-i}(\omega)]\cdot l}, \quad (15)$$

where $[\gamma_{mod-i}(\omega)] = \sqrt{[Y_{mod-i}(\omega)] \cdot [Z_{mod-i}(\omega)]}$ and l is the power cable length.

B. Synthesis of the Rational Functions

One of the problems encountered in power cable systems modeling is the accurate inclusion of frequency dependent effects in the time domain simulation. One successful solution is the representation of the system response throughout rational functions of low order [10]. Several techniques can be used to synthesize the rational functions and herein it is utilized the vector fitting method [24]. This method is based on the approximation in two stages, both with known poles. The first stage is carried out with real poles distributed over the frequency range of interest. In addition, an unknown frequency dependent scaling parameter is introduced which permitted the scaled function to be accurately fitted with prescribed poles. From the fitted function a new set of poles is obtained and then it is used in the second stage fitting the not-scaled function. This procedure was very successful in fitting the smooth functions that occurs in the cable modeling.

On this way, the rational functions are utilized to obtain the characteristic impedance and the propagation factor in the modal domain, represented in the *s-plane* by equations (16) and (17), allowing the transition from the frequency domain to time domain.

$$Z_{c-mod-(ij)}(s) \approx f(s) = \sum_{n=1}^{N} \frac{c_n}{s-a_n} + d + sh, \quad (16)$$

where $h = 0$ and $d \neq 0$.

$$A_{mod-(ij)}(s) = f(s) = \sum_{n=1}^{N} \frac{c_n}{s-a_n} + d + sh, \quad (17)$$

where $h = 0$ and $d = 0$.

The computer code is in the public domain, available from Gustavsen [24].

C. Implementation of the system in the time domain

After obtaining the rational functions of the characteristic impedance and the propagation factor, the next step is to implement the model in the time domain. Herein, it is utilized the PSCAD/EMTDC software, which is a commercial available program. The idea is to implement the developed model of the power cable in the PSCAD platform and to use all its routines to calculate the electromagnetic transients.

The main goal is change the data arquive that contains the results calculated takes into account the original cable model for the results that takes into account the power cable present in this paper.

Thus, after made this change it is necessary to run the PSCAD/EMTDC software using the DOS interface, as shown in the Figure 2:

Fig. 2. DOS interface utilized to run the $PSCAD/EMTDC^{©}$ program.

The PSCAD/EMTDC software carried out the results in the arquive "*.out" that can be easily read by other software, such as $MATALB^{©}$.

III. Computational Model Validation

With the objective to validate the proposed model several tests were realized in laboratory for a well known situations. The following voltage pulse propagation characteristics were analyzed in simulation and experimental analysis: zero-mode propagation, over-head propagation, induced voltages between conductors, short-circuited in one end. In this paper, it is presented the results for zero-mode and over-head voltage pulse propagation. Figure 3 shows the test setup that was utilized to verify the zero-mode propagation and Figure 4 shows the simulation and the experimental results. One can verify that the proposed model gives very well behavior results comparing to the experimental results. Figures 5 and 6 shows respectively the test setup and the simulation and experimental results for the over-head voltage pulse evaluation. Again, the proposed model has given very accurate results.

IV. Analysis of Overvoltage Phenomena

Several simulation and experimental tests were realized. Here in it is shown the overvoltage results for an induction motor drive when a power cable of 20 meters connects drive and motor. The power cable is placed in over-head trays (Figure 7). The proposed model was also implemented in the PSCAD software to analyze the overvoltage phenomena. The following are the drive system characteristics:

- 3 hp Inverter drive with a 330V DC bus;
- 150 nanoseconds voltage pulse rise time;
- 3 hp, 220/380V GE induction motor;
- 4 mm^2 four-wire cable with 20 meters length.

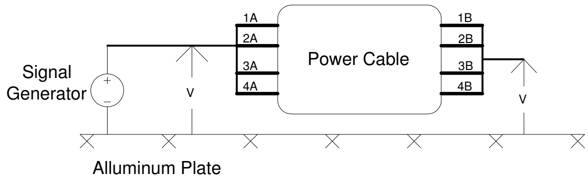

Fig. 3. Setup utilized for zero-mode propagation evaluation.

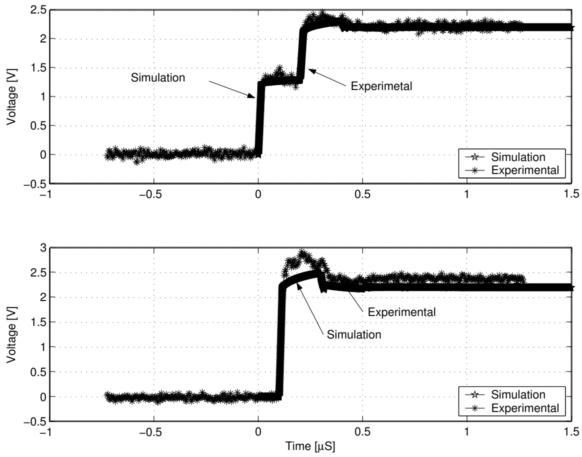

Fig. 4. Voltage measurements at the input and output of a $1,5mm^2$ power cable. Upper curve: measurements at the input. Lower curve: measurements at the output.

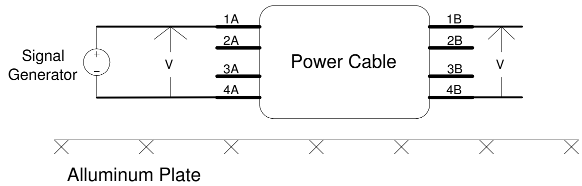

Fig. 5. Setup utilized for overhead-mode propagation evaluation.

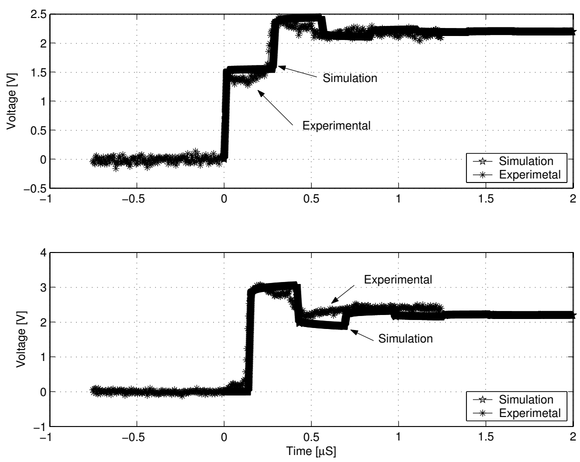

Fig. 6. Voltage measurements at the input and output of a $1,5mm^2$ power cable. Upper curve: measurements at the input. Lower curve: measurements at the output.

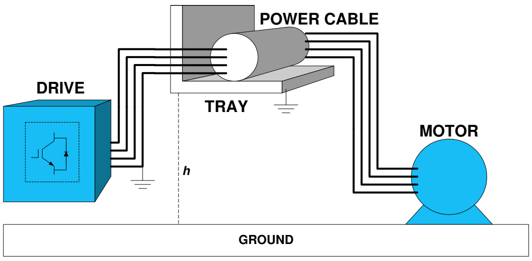

Fig. 7. Test setup for overvoltage analysis in long cable drives with the power cable placed over-head trays.

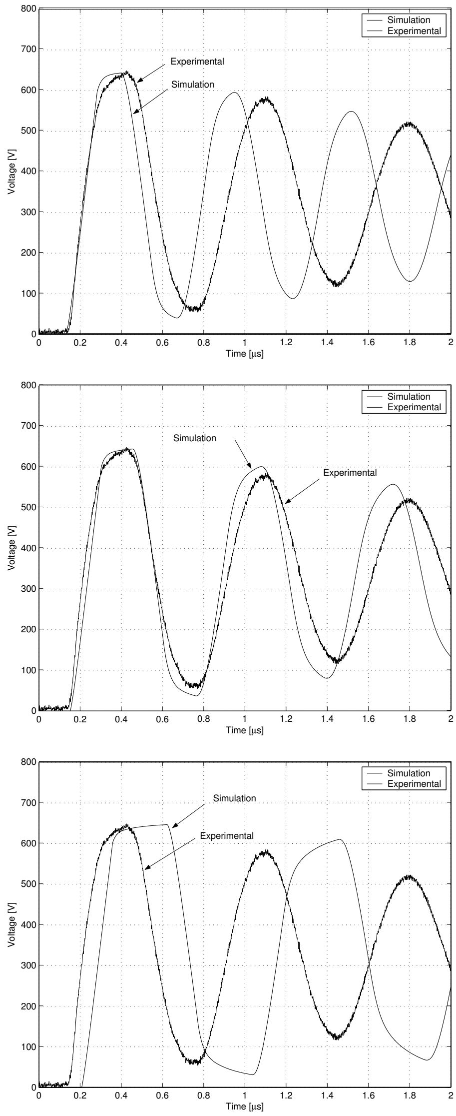

Fig. 8. Overvoltage analysis in a 3 hp induction motor drive for various values of relative permittivity. All curves are voltage waveforms at the cable end. Ground resistivity is approximately zero. Upper plot: $\epsilon_r = 1.9$. Middle plot: $\epsilon_r = 2.6$. Lower plot: $\epsilon_r = 5.1$.

Two groups of tests were realized varying the ground resistivity and the relative permittivity of the power cable wire insulator. The first group (Figure 8) shows the simulation

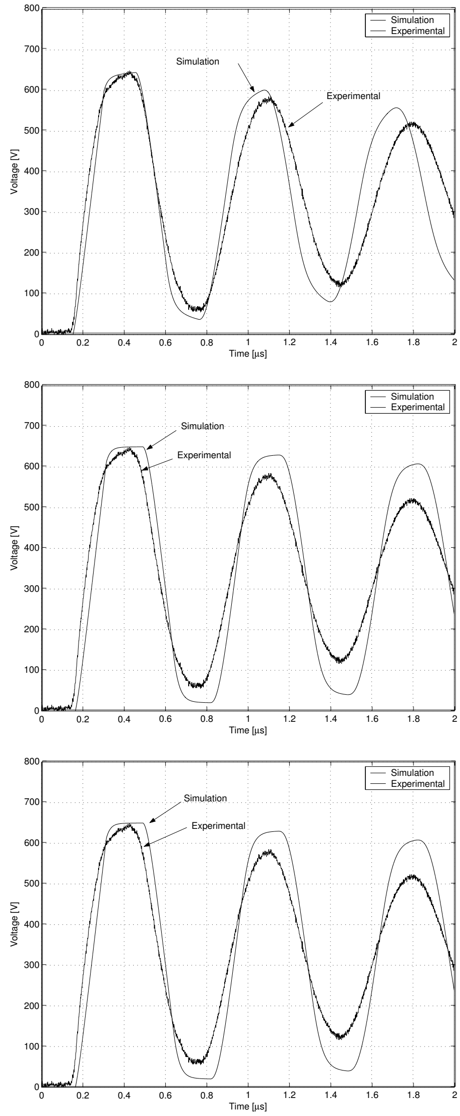

Fig. 9. Overvoltage analysis in a 3 hp induction motor drive for various values of ground resistivity in $\Omega.m$. All curves are voltage waveforms at the cable end. Relative permittivity is fixed in 2.6. Upper plot: $\rho_{ground} = 0$. Middle plot: $\rho_{ground} = 50$. Lower plot: $\rho_{ground} = 100$.

and experimental results of the overvoltage phenomena for various numbers of the relative permittivity, fixing the ground resistivity in approximately zero ($\rho_{ground} \approx 0\Omega.m$). Two conclusions can be obtained. First, the proposed model can successfully represent the overvoltage phenomena. One can verify that both voltage peaks and damping characteristics are very well represented. Second, the computational model is very dependent on the value of the relative permittivity of the power cable wire insulator. The best results are achieved with the value $\epsilon_r = 2.6$.

The second group of curves (Figure 9) show the simulation and experimental results of the overvoltage phenomena for various numbers of the ground resistivity, fixing the relative permittivity in 2.6 ($\epsilon_r = 2.6$). Again, one can verify the suitability of the model in representing the overvoltage phenomena. In this last case, an increasing of the ground resistivity increases significantly the travel time of the voltage pulse.

V. Conclusions

This paper has presented a power cable model to be implemented in PSCAD/EMTDC software for drive applications. Expressions to estimate series impedance, shunt admittance, characteristic impedance and propagation factor in the modal domain were developed based on the geometric and physical characteristics of the cable. Rational function were obtained using vector fitting approximation to realize the transition between the frequency domain to the time domain. This is an important contribution for the overvoltage analysis in long cable PWM drives because it allows one to use a professional platform to study the overvoltage phenomena, the PSCAD/EMTDC software, through a cable model with distributed nature including the dependence with frequency.

Simulation and experimental analysis were presented demonstrating that the proposed model can accurately represent the propagation characteristics of the voltage pulse. Overvoltage phenomena were analyzed in a 20 meters / 3 hp drive system and the experimental results corroborate the simulation ones. Another important conclusion is that the computational model is very sensitive with the relative permittivity of the power cable wire insulator and the correct choice of the ground resistivity allows one to have accurate results on the voltage pulse travel time.

Acknowledgment

The authors would like to thank the Laboratório de Aplicações Industriais and the Laboratório de Extra-Alta Tensão of the Departamento de Engenharia Elétrica, UFMG, which have supported this work.

References

[1] E. Persson. “Transient Effects in Applications of PWM Inverters to Induction Motors”. *IEEE Transactions on Industry Applications*, 28(5):1095–1101, Sep/Oct 1992.

[2] Austin Bonnett. “Analysis of the Impact of Pulse-Width Modulated Inverter Voltage Waveforms on AC Induction Motors”. *IEEE Transactions on Industry Applications*, 32(2):386–392, March/April 1996.

[3] G. Skibinski, D. Leggate, and R. Kerkman. “Cable Characteristics and Their Influence on Motor Over-voltage”. In *IEEE Applied Power Electronics Conference and Exposition*, volume 1, pages 114–121, Atlanta, GA, USA, 1997.

[4] R. Kerkman, D. Leggate, D. Schlegel, and G. Skibinski. “PWM Inverters and Their Influence on Motor Over-voltage”. In *IEEE Applied Power Electronics Conference and Exposition*, volume 1, pages 103–113, Atlanta, GA, USA, 1997.

[5] J. M. Bentley and P. L. Link. “Evaluation of Motor Power Cables for PWM AC Drives”. *IEEE Transactions on Industry Applications*, 33(2):342–358, March/April 1997.

[6] G. Skibinski. “Design Methodology of a Cable Terminator to Reduce Reflected Voltage on AC motors”. In *IEEE Industry Application Society Annual Meeting*, volume 1, San Diego, CA, USA, 1996.

[7] A. von Jouanne and P. N. Enjeti. “Design Considerations for an Inverter Output Filter to Mitigate the Effects of Long Motor Leads in ASD Applications”. *IEEE Transactions on Industry Applications*, 33(5):1138–1145, September/October 1997.

[8] A. F. Moreira, P. M. Santos, T. A. Lipo, and G. Venkataramanan. Filter networks for long cable drives and their influence on motor voltage distribution and common-mode currents. *IEEE Transactions on Industrial Electronics*, 52(2):515–522, April 2005.

[9] A. F. Moreira, T. A. Lipo, G. Venkataramanan, and S. Bernet. High-frequency modeling for cable and induction motor overvoltage studies in long cable drives. *IEEE Transactions on Industry Applications*, 38(5):1297–1306, September/October 2002.

[10] J. R. Marti. Accurate modeling of frequency-dependent transmission lines in electromagnetic transients simulations. *IEEE Transactions on Power Apparatus and Systems*, 101(1):147–157, January 1982.

[11] J. R. Marti. “Simulation of Transients in Underground Cables with Frequency-Dependent Modal Transformation Matrices”. *IEEE Transactions on Power Delivery*, 3(3):1099–1110, July 1988.

[12] A. Abur, O. Ozgun, and F. H. Magnano. “Accurate Modeling and Simulation of Transmission Line Transients Using Frequency Dependent Modal Transformations”. In *IEEE Power Engineering Society Winter Meeting)*, volume 2, pages 1443–1448, USA, 2001.

[13] A. Morched, B. Gustavsen, and M. Tartibi. A universal model for accurate calculation of electromagnetic transients on overhead lines and underground cables. *IEEE Transactions on Power Delivery*, 14(3):1032–1038, July 1999.

[14] B. Gustavsen. “Frequency-Dependent Transmission Line Modeling Utilizing Transposed Conditions”. *IEEE Transactions on Power Delivery*, 17(3):834–839, july 2002.

[15] Manitoba HVDC Research Centre, Winnipeg, Manitoba, Canada. *PSCAD/EMTDC Getting Started: Basics and Installation*, 2000.

[16] H. W. Dommel. *Electromagnetic Transients Program Reference Manual - EMTP Theory Book*. Department of Eletrical Engineering, The University of British Columbia, Vancouver, 1996.

[17] A. E. A. de Arajo and W. L. A. Neves. *Clculo de Transitrios Eletromagnticos em Sistemas de Energia*. Editora UFMG, 2005.

[18] A. Semlyen. Time domain modelling of frequency dependent three-phase transmission line impedance. *IEEE Transactions on Power Apparatus and Systems*, PAS-104(6):1540–1555, June 1985.

[19] J. R. Carson. Wave propagation in overhead wires with ground return. *Bell System Technical Journal*, 5:539–554, 1926.

[20] M. D'Amore and M. S. Sarto. A new formulation of lossy ground return parameters for transient analysis of multiconductor dissipative lines. *IEEE Transactions on Power Delivery*, 12(1):303–313, January 1997.

[21] H. de Paula. *Uma Nova Metodologia para a Determinao das Sobretenses Diferenciais e Correntes de Modo-Comum em Sistemas de Acionamemto de Motores de Induoi Atravs de Inversores PWM*. PhD thesis, Universidade Federal de Uberlndia, Uberlndia - Minas Gerais, Junho 2005.

[22] A. B. Fernandes and W. L. A. Neves. Frequency-dependent transformation matrices for phase-domain transmission line models. In *IEEE Power Engineering Society Summer Meeting*, volume 3, pages 1782–1787, July 2001.

[23] A. Deri, G. Tevan, A. Semlyen, and A. Castanheira. The complex ground return plane: A simple model for homogeneous and multi-layer return. *IEEE Transactions on Power Apparatus and Systems*, 8(PAS-100):3686–3693, August 1981.

[24] B. Gustavsen and A. Semlyen. Rational approximation of frequency domain responses by vector fitting. *IEEE Transactions on Power Delivery*, 14(3):1052–1061, July 1999.